^{11}B and ^{195}Pt NMR study of heavy-fermion compound $CePt_2B_2C$

2009 J. Phys.: Condens. Matter 21 415602

(http://iopscience.iop.org/0953-8984/21/41/415602)

J. Phys.: Condens. Matter **21** (2009) 415602 (6pp) doi:10.1088/0953-8984/21/41/415602

^{11}B and ^{195}Pt NMR study of heavy-fermion compound $CePt_2B_2C$

R Sarkar[1], A Ghoshray[1,3], B Pahari[1], M Ghosh[1], K Ghoshray[1], B Bandyopadhyay[1], M Majumder[1], V K Anand[2] and Z Hossain[2]

[1] Experimental Condensed Matter Physics Division, Saha Institute of Nuclear Physics, 1/AF Bidhannagar, Kolkata 700064, India
[2] Department of Physics, Indian Institute of Technology, Kanpur 208016, India

E-mail: amitabha.ghoshray@saha.ac.in

Received 16 May 2009, in final form 6 September 2009
Published 24 September 2009
Online at stacks.iop.org/JPhysCM/21/415602

Abstract

We report ^{11}B and ^{195}Pt NMR Knight shift K and spin–lattice relaxation rate $1/T_1$ in $CePt_2B_2C$ in the range 4–315 K. The quadrupolar coupling constant, ν_Q for boron nuclei is 790 ± 10 kHz. The change of hyperfine field, H_{hf}, is observed below 30 K in the K versus susceptibility, χ, plot. The calculated value of H_{hf} at the ^{11}B (^{195}Pt) is 0.156 (6.86) kOe/μ_B in the range 30–300 K and ∼0 (0.22) kOe/μ_B below 30 K. The $1/T_1$ versus T curve shows some exotic behavior. The Ce 4f spin contribution to the nuclear relaxation rate ($1/T_{1f}$) in each case is obtained by subtracting the T_{1K}^{-1} estimated from its La analog, i.e. $LaPt_2B_2C$. In the case of ^{11}B resonance, in the temperature range of 300–100 K, ($1/T_{1f}$) is independent of T, suggesting a Curie–Weiss behavior of the imaginary part of the dynamic susceptibility. It then shows a slow but continuous increment in the range 100–70 K, indicating a signature of the development of short-range magnetic correlation among the Ce 4f spins. Below 70 K, this enhancement of $1/T_{1f}$ is completely suppressed and it decreases sharply, indicating a suppression of the effect of magnetic correlation, due to the dominance of the Kondo effect over the RKKY interaction. $1/T_{1f}$, follows $\sim T^{\alpha}$, with an exponent $\alpha \sim 0.7$ in the range 4–30 K for ^{195}Pt and in the range 8–30 K for ^{11}B resonance. This is a characteristics of a non-Fermi-liquid like behavior. However, in the case of ^{11}B, there is again a clear change in the slope of the $1/T_{1f}$ versus T curve below 8 K, with the value of $\alpha = 1.0$, as if the behavior of the conduction electrons approaches towards a Fermi liquid, when probed near the ^{11}B site.

(Some figures in this article are in colour only in the electronic version)

1. Introduction

The quaternary borocarbides RPt_2B_2C (R = La, Ce, Pr) deserve particular attention because of their interesting physical properties. In this series, superconductivity was observed in $LaPt_2B_2C$ and $PrPt_2B_2C$ but not in $CePt_2B_2C$ [1, 2]. However, the Pt-based borocarbides have not been investigated as much as the Ni-based borocarbides because the former is difficult to prepare as a single-phase sample. As an example we refer to the paper by Kumagai *et al* [3], where ^{11}B and ^{195}Pt nuclear magnetic resonance (NMR) results clearly show the existence of a second phase having at least 30% of volume fraction. Hossain *et al* [2] later reported the formation of a heavy-fermion state in $CePt_2B_2C$ without any magnetic ordering down to 2 K. Kondo temperature was estimated to be $T_K \approx 30$ K. Since this sample had a 15% impurity phase, electronic properties at low temperature (<8 K) could not be determined accurately.

Better quality of samples, using a combination of arc melting and induction heating, were obtained by Anand *et al* [4]. The resistivity and specific heat of $CePt_2B_2C$ were found to be similar to those of $YbRh_2Si_2$ [4, 5] that shows non-Fermi-liquid (NFL) behavior due to its proximity to a quantum phase transition. Between 2 and 10 K, the electrical resistivity ρ of $CePt_2B_2C$ is linear in T, i.e. $\rho \approx \rho_0 - AT$, the zero-field electronic specific heat C_P varies

[3] Author to whom any correspondence should be addressed.

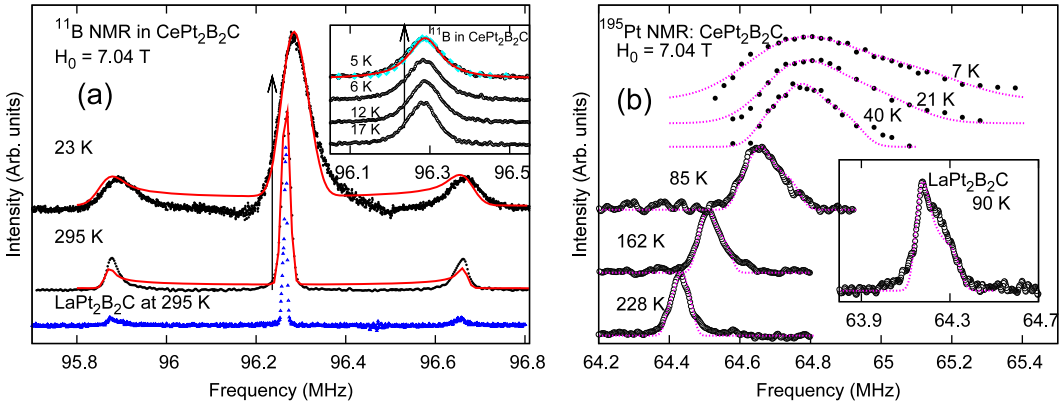

Figure 1. (a) ^{11}B NMR spectra of $CePt_2B_2C$ at 295 and 23 K. Simulated powder pattern is also shown. ^{11}B NMR spectra of $LaPt_2B_2C$ at 295 K is at the bottom. Inset shows FFT spectra of the $1/2 \rightleftharpoons -1/2$ transition showing temperature-independent linewidth at low temperature. Frequency swept spectrum and its theoretical fit are also shown superimposed on the FFT spectrum taken at 5 K. The arrow in each case represents reference position. (b) ^{195}Pt NMR spectra of $CePt_2B_2C$ at different temperatures. ○: FFT spectra, ●: frequency-swept spectra. Simulated powder pattern (dotted line) is also shown. Inset shows a typical ^{195}Pt NMR spectrum of $LaPt_2B_2C$ taken at 90 K.

as $-T \ln T$ and the Sommerfeld coefficient, γ, at 2 K is $\sim$0.3 J mol^{-1} K^{-2} [4]. Thus the temperature dependence of transport and thermal properties established this compound as a heavy-fermion system. The inverse magnetic susceptibility, χ^{-1}, also follows the Curie–Weiss law in the range 100–350 K with $\mu_{\rm eff} = 2.52\ \mu_{\rm B}$ and $\theta_P = -60$ K. The large absolute value of θ_P is an indication of strong hybridization of the Ce f electrons with conduction electrons. Finally, it was thought that the suppression of the superconductivity, expected at 8 K, is due to the presence of Kondo effect/heavy-fermion behavior. Since heavy-fermion compounds can exhibit unusual superconductivity, it demands further microscopic measurements like ligand site NMR.

In general, NMR can shed light on the microscopic magnetic and electrical properties by analyzing the temperature variation of the Knight shift K and spin–lattice relaxation rate $1/T_1$. K gives information about the uniform static spin susceptibility χ' (if $q = 0$) and $1/T_1T$ reveals the spin-fluctuation character from the **q** averaged dynamical spin susceptibility $\chi''(q, \omega)$. In the conventional Fermi liquid state, both K and $1/T_1T$ are T-independent and obey the Korringa relation. Deviation from the Korringa relation indicates the presence of the magnetic correlations in the material. In order to understand the low temperature electronic state we have performed both ^{11}B and ^{195}Pt NMR using the same lot of the sample of $CePt_2B_2C$ on which thermal and transport properties were measured [4]. As a reference material, we have also performed ^{11}B and ^{195}Pt NMR on a relatively pure sample of $LaPt_2B_2C$. It may be mentioned that NMR of a ligand nucleus has a drawback in the difficulty in quantitative analysis of the transferred hyperfine coupling at the ligand site. However, this study directly probes the hybridization of the f electrons with ligand electrons, which play the dominant role in determining the electronic properties of the f-electron system. A preliminary ^{11}B NMR result in $CePt_2B_2C$ has been presented in [6].

2. Experimental details

The polycrystalline sample of $CePt_2B_2C$ was prepared as mentioned in [4]. ^{11}B and ^{11}Pt NMR experiments were performed in an external magnetic field of 7.04 T using a conventional phase coherent spectrometer. Spin-echo signals were measured by applying a $\pi/2$–τ–$\pi/2$ solid echo sequence and, in the case of narrow lines, spectra were obtained by fast Fourier transform (FFT). The relatively broad signal was obtained by scanning the spectrometer frequency. The nuclear spin–lattice relaxation times, T_1, were obtained by the saturation recovery method. Temperature variation was achieved in an Oxford cryostat with an ITC 503 temperature controller in the range 4–315 K.

3. Results and discussion

3.1. Spectral features of ^{11}B and ^{195}Pt NMR

The tetragonal crystal structure (space group: $I4/mmm$) of $CePt_2B_2C$ consists of a sequence of Ce–C, B, Pt, B and Ce–C layers. Four equivalent B sites have axial symmetry and Pt (four equivalent) sites are non-axial. The ^{11}B NMR spectrum shows the typical pattern expected for a powder sample of spin $I = 3/2$, which consists of a central transition and a pair of satellites. Figure 1(a) shows two such spectra observed at 295 and 23 K. Though the linewidths of the central and the satellite lines increase substantially at low temperatures, the features of anisotropy typical of a powder pattern are not discernible. Nevertheless, we have analyzed the spectra by simulation of the powder pattern considering complete anisotropy in magnetic and quadrupolar interaction. Reasonably good simulated spectra are also shown in figure 1(a). This provides accurate values of the shift and quadrupolar interaction parameters. In the case of $CePt_2B_2C$, we obtain a quadrupolar coupling constant, $\nu_{\rm Q} = 790 \pm 10$ kHz (the same as estimated from the satellite pair separation) and the asymmetry parameter, η, is zero. The almost-temperature-independent behavior of $\nu_{\rm Q}$ excludes the possibility of any lattice distortion throughout the measured temperature range. Figure 1(a) also shows a ^{11}B NMR spectrum of $LaPt_2B_2C$ as reference and for this sample $K_{\rm iso} = 0.032\%$ and $\nu_{\rm Q} = 780 \pm 10$ kHz with $\eta = 0.0$. However, we did not observe

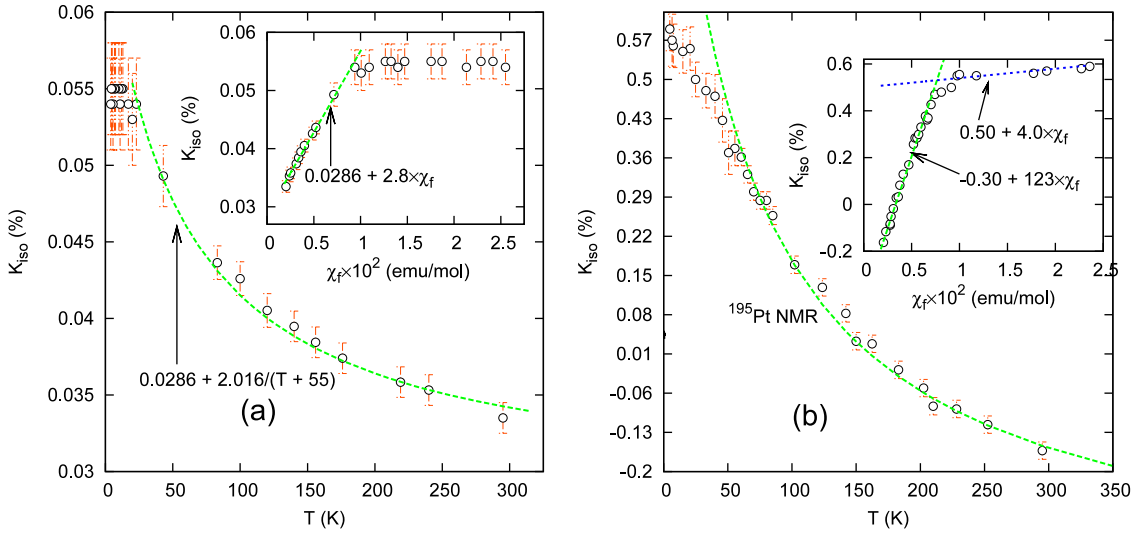

Figure 2. Variation of $K_{\rm iso}(\%)$ with T and χ_f for (a): ^{11}B NMR; (b): ^{195}Pt NMR in $CePt_2B_2C$. Theoretical lines have been explained in the text.

any signal arising from the second phase as was observed by Kumagai *et al* [3] confirming the better quality of our sample.

In the inset of figure 1(a), only the central transition of ^{11}B FFT spectra for $CePt_2B_2C$ below 20 K has been shown. The frequency-swept spectrum obtained at 5 K has also been shown superimposed on the FFT spectrum to show that $\pi/2$ pulse length has been correctly set to observe the whole range of the spectrum in each case. The most important observation in the range 5–17 K is that the peak position and the linewidth are roughly temperature-independent. However, it seems surprising that the resonance spectrum has a Lorentzian shape, instead of the more likely Gaussian form. One such theoretical fit (at 5 K) with $K_{\rm iso} = 0.055\%$, $K_{\rm an} = 0.001\%$ and $K_{\rm ax} = 0.005\%$ has been shown by the continuous line. The anisotropic shift at the boron site being small, we will discuss only the temperature variation of the isotropic Knight shift $K_{\rm iso}$ in the following section.

Figure 1(b) shows the ^{195}Pt NMR spectrum of $CePt_2B_2C$ along with the simulated pattern. The spectrum consists of a powder pattern observed for a nuclear spin $I = 1/2$ with a large anisotropic frequency shift. Below 40 K, lines broaden excessively. Therefore, only the frequency-swept spectra have been measured. All the shift parameters, i.e. $K_{\rm iso}$, $K_{\rm an}$ and $K_{\rm ax}$ show considerable temperature dependence down to 20 K, below which they are almost temperature-independent, as in the case of ^{11}B NMR. Moreover, in the case of $LaPt_2B_2C$ (a typical spectrum at 90 K is shown in the inset of figure 1(b)), the shift parameters have little temperature dependence. We should mention that we did not observe any signal from other phases as was observed by Kumagai *et al* [3].

3.2. *Knight shift of* ^{11}B *and* ^{195}Pt

Figure 2 shows the temperature dependence of the ^{11}B and ^{195}Pt Knight shift $K_{\rm iso}$, respectively. Pt and B nuclei can be regarded as belonging to ligand sites, which have no intrinsic magnetic moments. In general, magnetic shift of the NMR lines is a sum of three contributions: $K = K_{\rm dia} + K_{\rm orb} + K_{\rm spin}$, where $K_{\rm dia}$ is the diamagnetic (or chemical) contribution due to inner electron shells, $K_{\rm orb}$ is the Van Vleck orbital contribution and $K_{\rm spin}$ is the Knight shift due to spin paramagnetism of the 2s and/or 2p electrons for ^{11}B and 6s and/or 5d electrons for Pt. All these contributions are temperature-independent (their sum is denoted as K_0, similar to χ_0 in the total magnetic susceptibility χ) which is a characteristic of the usual Pauli paramagnetic metals like $LaPt_2B_2C$. In the case of $CePt_2B_2C$, the additional contribution to $K_{\rm spin}$ is $K_{\rm s-f}$ which arises due to the polarization of the conduction electrons due to s–f exchange (RKKY) interaction and is temperature-dependent and proportional to $\chi_f(T)$. Thus, the most general expression for K is

$$K = K_0 + \frac{H_{\rm hf}(f)}{N\mu_{\rm B}}\chi_f, \qquad (1)$$

where $H_{\rm hf}(f)$ is the hyperfine field due to 4f electrons. As long as $H_{\rm hf}$ is independent of temperature, $K_{\rm spin}$ is proportional to χ. It is seen from figure 2 that $K_{\rm iso}$ versus T curves in the range 25–300 K were fitted theoretically (dotted lines) using the Curie–Weiss expression for $\chi_f(T)$ in equation (1). These curves give $K_0 = 0.029\%$ and -0.3% for ^{11}B and ^{195}Pt nuclei, respectively, with $\theta = -55$ K and the product of the Curie constant C and $H_{\rm hf}$.

The insets of figure 2 show the $K_{\rm iso}$ versus $\chi_f = \chi - \chi_0$ plot for ^{11}B and ^{195}Pt NMR in $CePt_2B_2C$, with temperature as an implicit parameter. Plots above 25 K follow a linear relation. The intercept gives $K_0 = 0.029\,(-0.3)\%$ for ^{11}B (^{195}Pt) nuclei and the slope of the dotted lines gives $H_{\rm hf} = 0.156$ kOe/$\mu_{\rm B}$ (6.86kOe/$\mu_{\rm B}$) for ^{11}B (^{195}Pt) nuclei. Similar values of K_0 had been reported by Kumagai *et al* [3] for $LaPt_2B_2C$. It should be stressed that the difference in the sign of K_0 for Pt as reported by them from that of the present one is due to the fact that we have used the sign of the low frequency shift as negative, whereas they used a positive sign for the same. These authors have discussed the different contributions to K_0. The same discussion is also valid for the $CePt_2B_2C$ case.

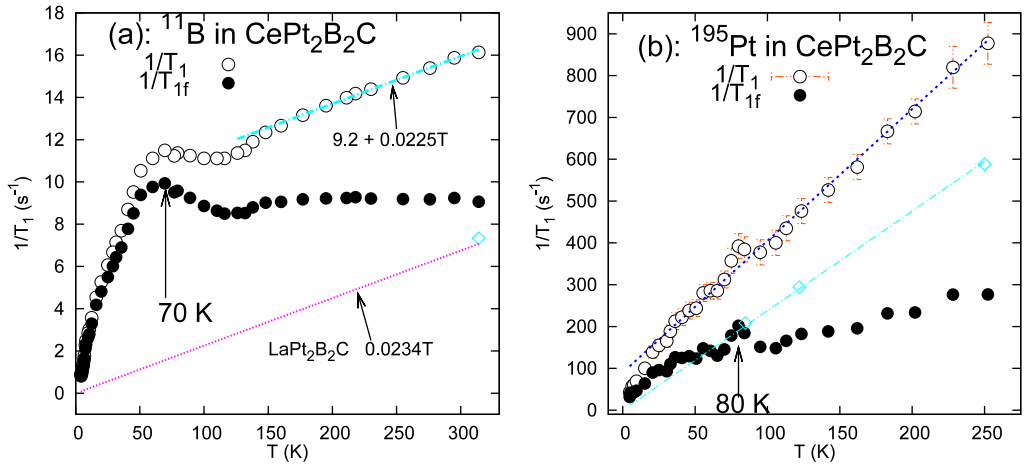

Figure 3. Temperature dependence of $1/T_1$ of (a) ^{11}B at 7.04 T for ○: $CePt_2B_2C$, ◇: $LaPt_2B_2C$ from experiment, · · · · · ·: $LaPt_2B_2C$ after simulating, ●: $1/T_{1f}$ obtained after subtracting Korringa contribution for $LaPt_2B_2C$ from experimental $1/T_1$ values of $CePt_2B_2C$. (b) ^{195}Pt at 7.04 T for ○: $CePt_2B_2C$, ◇: $LaPt_2B_2C$, · · · · · ·: $LaPt_2B_2C$ after simulating, ●: $1/T_{1f}$.

The transferred hyperfine mechanism between f electrons and the ligand site is achieved via the conduction electrons. The strong site dependence of H_{hf} originates from the localized f-electron configuration affecting the hybridization of the f moments and the ligand electrons. H_{hf} at the B site originates from transferred hyperfine couplings with 4f spin of the four neighboring Ce ions ($z = 4$) and should be reduced to the transferred hyperfine field of $H_{hf} = 0.039$ kOe/μ_B per Ce ion. The same in the case for Pt, which is bonded with two Ce ions, is 3.43 kOe/μ_B. Using the value of H_{hf}, the Curie constant (C) is determined from the product of C and H_{hf} obtained from simulation of K_{iso} versus T curves. This agrees quite satisfactorily with that of trivalent cerium. An order-of-magnitude larger value of H_{hf} for Pt compared to that of B should make it more sensitive in detecting the change in the low temperature electronic state. Indeed, this is reflected in the low temperature lineshape of Pt.

Below 25 K, the K_{iso} versus χ_f plot deviates from linearity, indicating a change of H_{hf}. Two different mechanisms have been proposed to explain this deviation in other heavy-fermion systems. In $CeSn_3$ the proportionality of K of Sn and χ starts to differ below 150 K, and this effect has been ascribed to the modifications of the effective hyperfine coupling at Sn (via the RKKY interaction) by the onset of Kondo compensation below T_K [7]. In $CeCu_2Si_2$, Ohama *et al* [8] observed that the shifts of Cu and Si exhibited departures from linearity in the K versus χ plot below 100 K with a change in the sign of the hyperfine coupling constant. They explained this behavior as due to the depopulation of an excited CEF level of the Ce ions ($J = 5/2$) and not arising from Kondo coherence. The overlap between the Ce 4f orbitals and the conduction electrons changed, depending on the CEF level populations, resulting in temperature-dependent hyperfine couplings to Cu and Si. The observed change in sign of H_{hf} was explained as due to the orbital overlap between the ligand s orbital and the Ce 4f orbital. They distinguished this direct transferred hyperfine mechanism from that in which the 4f moment polarizes the conduction band at the Ce site. According to Ohama *et al*, the direct contribution can become negative when only the lowest CEF doublet is occupied. In the present case, the magnitude of $H_{hf}(f)$ becomes ∼0 for B and 0.22 kOe/μ_B for Pt resonances below 25 K. The existence of a small but non-zero H_{hf} for the Pt nucleus ensured that the resonance lineshape could still sense the influence of the reduced 4f moment in the Kondo compensated regime (below 25 K) through an increase in linewidth, whereas B could not. Normally during gradual compensation of the 4f moment below T_K, no enhancement of the resonance linewidth is expected, similar to that observed for the ^{27}Al NMR linewidth below T_K (100 K) in another non-magnetic dense Kondo compound $CeNiAl_4$ [9]. Indeed, in the case of the ^{11}B resonance, the linewidth remains constant below ∼20 K (inset of figure 1(a)). However, this is not the case for ^{195}Pt resonance. The role of 5d electrons for ^{195}Pt may not be ruled out. Possibly it could be a reason for the absence of superconductivity in this compound. Thus an extension of NMR studies to further lower temperature using a single crystal is desirable.

3.3. Nuclear spin–lattice relaxation time, T_1

T_1 of ^{11}B was measured by saturating the central line of the quadrupole powder pattern spectrum with a single $\pi/2$ pulse and monitoring the growth of the solid echo at variable delays. The value of T_1 was extracted by fitting the decay curve of the nuclear magnetization to the recovery law:

$$M(\infty) - M(t) = M(\infty)C[0.1\exp(-t/T_1) + 0.9\exp(-6t/T_1)]. \quad (2)$$

Temperature dependence of $1/T_1$, as shown by the open circle (○) in figure 3(a) clearly shows three changes in the slope of the rate curve. $1/T_1$ continuously decreases linearly down to 150 K, it shows a plateau in the range of 130–70 K and then again decreases sharply in the range 4–70 K.

In addition to the Korringa relaxation rate, T_{1K}^{-1}, which is usually observed in normal metals (e.g. $LaPt_2B_2C$) without

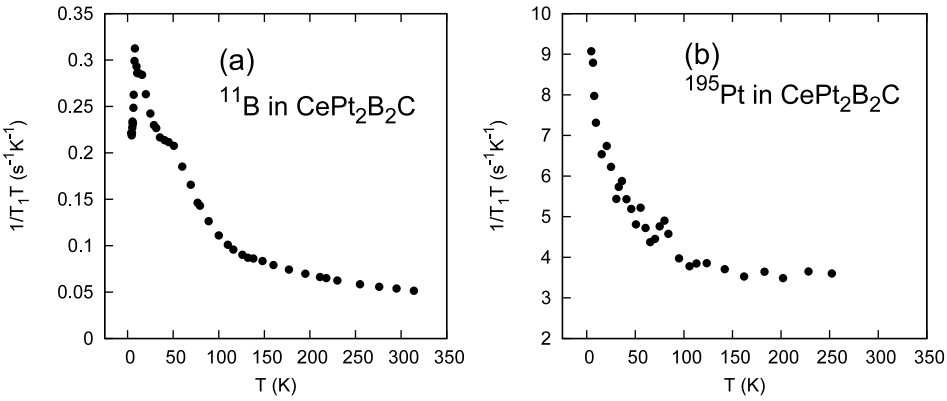

Figure 4. Temperature dependence of $1/T_1T$ in $CePt_2B_2C$: (a) ^{11}B, (b) ^{195}Pt.

localized magnetic moments, the experimental $1/T_1$ in $CePt_2B_2C$ would be enhanced due to spin-fluctuation effects as given by [10]

$$T_1^{-1} = T_{1K}^{-1} + T_{1f}^{-1}. \tag{3}$$

T_{1K}^{-1} depends linearly on T and the proportionality constant depends on the transferred hyperfine coupling, A_{hf}, and density of electronic states at the Fermi level. This provides access to the hybridization-enhanced density of states at the Fermi level for heavy-fermion systems. The term T_{1f}^{-1} is due to spin fluctuations that will be transferred via the RKKY interaction from the local moments to the site of the NMR nucleus. Considering the low number of nearest cerium atoms (four in the case of the boron atom), following Büttgen *et al* [11], one can write

$$T_{1f}^{-1} \propto \frac{k_B T}{\omega_0} \operatorname{Im} \chi(\omega_0, T), \tag{4}$$

where ω_0 is the frequency of the NMR experiment.

The Korringa contribution in the case of ^{11}B nuclei of $CePt_2B_2C$ is obtained from the linear relation of $1/T_1$ (dotted line in figure 3) in the temperature range 300–150 K. The Korringa constant 0.0225 s^{-1} K^{-1} that matches very well with that for $LaPt_2B_2C$ [3] (also from experiment at 295 K) is found to be an order of magnitude smaller than that of other heavy-fermion compounds like $CeCu_2Si_2$ (0.6 s^{-1} K^{-1}) and $YbAgCu_4$ (5.9 s^{-1} K^{-1}).

The variation of $1/T_{1f}$, obtained by subtracting the Korringa contribution from the total $1/T_1$, is also shown in figure 3. In the range 300–100 K, $1/T_{1f}$ is independent of T, indicating that the dynamical susceptibility follows the Curie–Weiss behavior suggesting that the rate is dominated by the fluctuation of Ce^{3+} moments. As the temperature is decreased, $1/T_{1f}$ starts to enhance slowly because of the development of short-range correlation between the Ce magnetic moments. However, below 70 K, $1/T_{1f}$ again decreases sharply, indicating the suppression of the short-range correlation effect and dominance of the Kondo effect, reducing the 4f spin contribution to the nuclear relaxation process due to the antiferromagnetic coupling of the 4f spin and the conduction electron spin. This is the Kondo temperature (maximum value in $1/T_{1f}$). Details of the Kondo compensated region would be discussed in subsection 3.3.1.

The decay of the ^{195}Pt nuclear magnetization follows a single exponential curve in the whole temperature range (4.7–250 K). Figure 3(b) shows the temperature dependence of $1/T_1$ in $CePt_2B_2C$ and $LaPt_2B_2C$. In $CePt_2B_2C$, $1/T_{1f}$ shows a weak temperature dependence in the range 100–250 K. Then there is a signature of enhancement in the temperature range ($T \approx 100$ K) as in the case of ^{11}B. However, the peak (80 K) is not prominent as in the case of ^{11}B.

Figure 4 shows the variation of $1/T_1T$ (i.e. absorptive part of the dynamic susceptibility from equation (4)) with T for ^{11}B and ^{195}Pt resonances in the whole temperature range. In both the cases $1/T_1T$ shows a weak increment in the range 100–250 K. In the case of ^{195}Pt, its value 3.5 s^{-1} K^{-1} is much smaller than the value of 33 s^{-1} K^{-1} in Pt metal [12]. Below 100 K, there is a continuous enhancement showing a small peak around 80 K, while in the case of ^{11}B, a similar enhancement (with a plateau around 50–70 K) is observed down to 7.5 K. The reason for a narrow peak (also found as the change in the slope of the $1/T_{1f}$ curve; to be discussed later) around 7.5 K is not clear. According to equation (4), $1/T_1T$ should follow the T dependence of the dynamic susceptibility. Thus one would be tempted to ascribe this as magnetic ordering in the Kondo compensated region. In $Ce(Cu_{0.3}Ni_{0.7})Ge_2$, such a type of peak at 2.5 K in the $1/T_1T$ curve has been interpreted as a signature of heavy-fermion band magnetism (HFBM) [11]. However, in neutron diffraction experiments, no indication of magnetic Bragg reflections could be detected [17].

Thus it is clear from figures 3 and 4 that the short-range correlation among the Ce 4f spins starts to develop near 100 K and continues till 70 K. Moment compensation begins from around 70 K (Kondo temperature). There is experimental evidence of the development of such short-range magnetic correlations in other Ce-based Kondo lattice systems such as $Ce_3Ir_2Ge_2$ [18] and $Ce(Cu_{0.3}Ni_{0.7})Ge_2$ [11] showing no long-range order. Such a possibility was discussed theoretically [19] by including the nearest-neighbor magnetic exchange interaction in the Kondo lattice model. It shows that magnetic correlations can appear at a temperature, T_{cor} which is larger than the Kondo temperature (T_K) and was observed experimentally, e.g. in $CeRu_2Si_2$ [20]. In our case $T_{cor} \sim 100$ K and $T_K \sim 70$ K. Thus we can conclude that $CePt_2B_2C$ lies in the border region between the

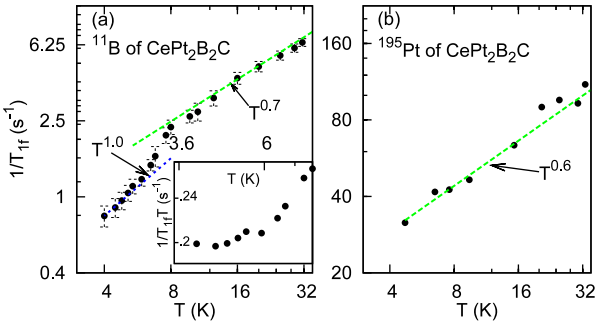

Figure 5. Temperature dependence of $1/T_{1f}$ of (a) ^{11}B and (b) ^{195}Pt for $CePt_2B_2C$. Dashed lines represent power law with exponent as shown in the figure. Inset in the left panel shows temperature dependence of $1/T_{1f}T$ showing a constant value of 0.22 s^{-1} K^{-1} below 6 K.

magnetic-RKKY-interaction-dominated regime and the pure non-magnetic Kondo region. The value of the Sommerfeld coefficient, γ (0.3 J mol^{-1} K^{-2}) indeed lies between 1 (non-magnetic) and 0.1 (magnetic) J mol^{-1} K^{-2}.

3.3.1. Non-Fermi-liquid behavior. Figure 5 shows the temperature dependence of $1/T_{1f}$ below 32 K for (a) ^{11}B and (b) ^{195}Pt in $CePt_2B_2C$. Generally, $1/T_{1f}$ follows power law behavior $T_{1f}^{-1} \sim T^{\alpha}$, where the exponent α is unity for a Fermi liquid (FL) model. Departure from unity indicates a non-Fermi-liquid (NFL) behavior. Theoretically, NFL behavior is expected to occur close to a quantum phase transition, but can also occur in multichannel Kondo systems [13, 14] or a distribution of Kondo temperatures [15, 16] or in impurity systems [21]. Tsvelik and Reizer [22] proposed a phenomenological theory for NFL-type features of heavy-fermion metals and suggested the value of this exponent to be 0.33. However, Sengupta and Georges [23] predicted that the value of α is ∼0.25. In the case of $CePt_2B_2C$, for ^{195}Pt resonance, we obtain $\alpha = 0.6$ in the range 4–30 K, whereas, for ^{11}B, $\alpha = 0.7$ in the regime 30–10 K and $\alpha = 1.0$ in the range 4–8 K. The values of the exponent obtained from the present ^{195}Pt NMR results and for ^{11}B above 8 K show considerable departure from theoretical predictions.

Interestingly, the normal FL-like behavior with $(T_{1f}T)^{-1} = 0.22$ s^{-1} K^{-1} (inset in figure 5) reappears at below 10 K when probed at the B site. The NMR results therefore suggest a modification of the electronic state below 30 K, resulting in an unusual value of α and a change in the hyperfine coupling constant (as revealed from the K versus χ plot).

4. Summary

^{11}B and ^{195}Pt NMR studies were performed in the range 4–315 K in a high purity sample of $CePt_2B_2C$, in which the resistivity and the specific heat results indicate a non-Fermi-liquid (NFL) behavior in the temperature range 2–10 K. The Knight shifts of both the resonances suggest a change in the hyperfine coupling constants H_{hf} below 30 K, indicating a modification of the conduction electron wavefunction due to s–f mixing. The Ce 4f spin contribution to the nuclear spin–lattice relaxation rates $1/T_{1f}$ shows the signature of the development of short-range correlation within the Ce 4f moments near 100 K, and this is again suppressed below 70 K due to the dominance of the Kondo effect. This finding corroborates the theoretical prediction [19] for Kondo systems. Moreover, $1/T_{1f}$ follows an NFL behavior in the range 4–30 K for ^{195}Pt and in the range 8–30 K for ^{11}B resonance with an exponent $\alpha \sim 0.7$. However, in the case of ^{11}B, there is again a clear change in the slope of the $1/T_{1f}$ versus T curve below 8 K, with the value of $\alpha = 1.0$, as if the behavior of the conduction electrons approaches towards an FL when probed near the ^{11}B site. A possible reason for ^{195}Pt to be insensitive to detecting the change from NFL to FL behavior may be the large anisotropic linewidth, which limits the accuracy of the measurement of relaxation time. This could arise from Pt 5d electrons, in addition to that due to Ce 4f electrons. Therefore, further study at low temperature with a good single crystal is essential to probe the origin of the strong anisotropic field at the Pt site.

References

[1] Cava R J, Batlogg B, Seigrist T, Krajewski J J, Peck W F Jr, Carter S, Felder R J, Takagi H and van Dover R B 1994 *Phys. Rev.* B **49** 12384
[2] Hossain Z, Geibel C, Gupta L C, Nagarajan R and Godart C 2002 *J. Phys.: Condens. Matter* **14** 7045
[3] Kumagai K, Ikeda S, Roos J, Mali M and Brinkmann D 1996 *Physica* C **272** 301
[4] Anand V K, Geibel C and Hossain Z 2007 *Physica* C **460–462** 636
[5] Trovarelli O, Geibel C, Mederle S, Langhammer C, Grosche F M, Gegenwart P, Lang M, Sparn G and Steglich F 2000 *Phys. Rev. Lett.* **85** 626
[6] Sarkar R, Ghoshray A, Pahari B, Ghoshray K, Anand V K and Hossain Z 2008 *CP1003 Magnetic Materials* p 213
[7] Kim E, Makivic M and Cox D L 1995 *Phys. Rev. Lett.* **75** 2015
[8] Ohama T, Yasuoka H, Mandrus D, Fisk Z and Smith J L 1995 *J. Phys. Soc. Japan* **64** 2628
[9] Ghoshray K, Bandyopadhyay B and Ghoshray A 2002 *Phys. Rev.* B **65** 174412
[10] Lysak M J and MacLaughlin D E 1985 *Phys. Rev.* B **31** 6963
[11] Büttgen N, Böhmer R, Krimmel A and Loidl A 1996 *Phys. Rev.* B **53** 5557
[12] Carter G C, Bennet L H and Kahan J D 1977 *Metallic Shifts in NMR 1* (Oxford: Pergamon)
[13] Nozieres P and Bladin A 1980 *J. Physique* **41** 193
[14] Cox D L 1987 *Phys. Rev. Lett.* **59** 1240
[15] Bernal O O, McLaughlin D E, Lukefahr H G and Andraka B 1995 *Phys. Rev. Lett.* **75** 2023
[16] Miranda E, Dobrosavljevic V and Kotliar G 1997 *Phys. Rev. Lett.* **78** 290
[17] Loidl A, Krimmel A, Knorr K, Sparn G, Lang M, Geibel C, Horn S, Grauel A, Steglich F, Welslau B, Grewe N, Nakotte H, de Boer F R and Murani A P 1992 *Ann. Phys.* **1** 78
[18] Li D X, Nimori S, Homma Y, Shiokawa Y, Tobo A, Onodera H, Haga Y and Onuki Y 2005 *J. Appl. Phys.* **97** 073903
[19] Iglesias J R, Lacroix C and Coqblin B 1997 *Phys. Rev.* B **56** 11820
[20] Kawsaki Y, Ishida K, Kitaoka Y, Asayama K, Nakamura H and Flouquet J 1999 *Physica* B **259–261** 77
[21] Bhatt R N and Fisher D S 1992 *Phys. Rev. Lett.* **68** 3072
[22] Tsvelik A M and Reizer M 1993 *Phys. Rev.* B **48** 9887
[23] Sengupta A M and Georges A 1995 *Phys. Rev.* B **52** 10295